Forces in Mechanics 13 (2023) 100233

Contents lists available at ScienceDirect

Forces in Mechanics

journal homepage: www.sciencedirect.com/journal/forces-in-mechanics

Comparison of the stress intensity factor for a longitudinal crack in an elliptical base gas pipe, using FEM vs. DCT methods

Luis Espinoza [a,*], Jose Antonio Bea [a], Sourojeet Chakraborty [b], Daniela Galatro [b]

[a] University of Zaragoza, C. de Pedro Cerbuna, 12, Zaragoza 50009, Spain
[b] Department of Chemical Engineering & Applied Chemistry, University of Toronto, ON M5S 3E5, Canada

ARTICLE INFO

Keywords:
Piping
Finite Element Method (FEM)
Stress intensity factor
Cracks propagation
Displacement Correlation Technique (DCT)

ABSTRACT

While several theoretical and experimental studies for cracks in piping exist, most pertain to pipelines, equipment, or fittings under pressure conditions or under stress corrosion conditions at welding. Element finite Method models have occasionally supplemented experimental methods, to investigate such operational fails. In this approach we explore technical options to comprehensively understand crack propagations, by first, evaluating the Stress Intensity Factor (K_I) using ANSYS Parametric design language then, comparing with the Displacement Correlation Technique, for an elliptical base gas piping (20″APL Gr. B) suffering a longitudinal welding-induced crack, under a compression of 1.86 MPa. The K_I value for an Electric Resistance Welding crack was calculated for the two-dimensional plane, for a quarter-length of propagated crack along the elliptical front. The K_I value estimates are $0.94x(10)^{-3}$ MPa$\sqrt{m}$ from ANSYS Parametric design language vs. $0.70x(10)^{-2}$ MPa$\sqrt{m}$ from DCT the two methods are close less than 1. These results were compared with the theorical stress intensity factor for elliptical cracks by Broek[1] David called elementary engineering fracture mechanics where the values were $0.5x(10)^{-1}$ MPa$\sqrt{m}$. We found that the proposed FEM method for estimating (K_I)is the approach that is closest to the theoretical value.

1. Introduction

Industrial fields like production, refining, and oil, gas, and derivatives transportation, commonly involve the flow of various complex fluids via piping systems, most commonly connected through Electric Resistance Welding (ERW). Such transport modes are known to lead to the occurrence of cracks, which have caused numerous accidents, primarily due to ERW induced pressure buildup in pipeline networks [1]. The Fig. 1 shows a quick look at incidents involving gas service pipelines, the so-called gas pipelines, presents some important numbers to analyses (according to the latest available EGIG report) [2].

Companies must be made aware that they must be at the forefront of changes in the way engineering is done, by applying scientific methods to crack propagation problems. The empirical must be overcome by integral solutions with technical foundations that guarantee to minimize:

- Human losses.
- Injuries to workers.
- Accidents in industrial installations.
- Environment.

In recent years, crack growth analyses have been necessary, and has been extensively investigated: for instance, Toribio, Gonzalez and Matos They proposed a review and synthesis of the stress intensity factor for elliptical surface cracks in round bars under tension. Their approach was only numerical, and they came to several conclusions, such as: The dimensionless stress intensity factor (SIF) increases with the relative crack depth (a/D), decreases with the crack aspect ratio (a/b) and changes continuously from the crack center to the crack surface, increasing or decreasing as a function of these two extreme values (center and surface) [3]. Branco, Costas and Antunes carried out a numerical and experimental analysis of the fatigue behavior of round bars with lateral notches under the action of loads where they obtained Finally, very good correlations between experimental and predicted fatigue lives were observed, particularly for lives greater than 104 cycles [4], Wojciech Macek at 2017 He also performed load cycling tests on

* Corresponding author.
E-mail address: 846552@unizar.es (L. Espinoza).

[1] Broek, D. (1984). Elementary engineering fracture mehcanics . The Hague: Martinus Nijhoff Publishers.

https://doi.org/10.1016/j.finmec.2023.100233
Received 7 June 2023; Received in revised form 22 August 2023; Accepted 1 September 2023
Available online 6 September 2023

List of symbols

K_I	stress intensity factor
ν	poisson's Coefficient / poisson's ratio
V_i	perpendicular displacements to the fissure plane
E	young's modulus
X,U	auxiliary dimensionless coordinate system
Y,V	auxiliary dimensionless coordinate system
L	length of the degenerated element
U,X	degree of freedom
U,Y	degree of freedom
ν	poisson's ratio/coefficient
σ_m	applied tensile stress
$E(k)$	the elliptic integral of the second kind
a	crack depth, half the minor axis of a semi-elliptical crack
c	half surface length or half the mayor axis of a semi-elliptical crack

List of abbreviations and subscripts

ERW	electrical resistance welding
TD	design temperature
PD	desing pressure
APDL	ANSYS parametric design language
DCT	displacement correlation technique
SIF	stress intensity factors
OA	segment OA of crack
USER	specific work units
HAZ	heat affected zone

fractured surfaces of aluminum alloys based on the available advantages of fractography [5]. Pinheiro and Pascualino evaluated fatigue lives of damaged pipes under internal pressure cycles [6], while Gates analyzed the growth behavior of fatigue cracks under variable amplitude loads [7]. To analyze and predict tensile fatigue behavior, one needs to know the Stress Intensity Factors (SIFs), along the crack. Over the years, several experimental tests conducted for various symmetrical and elliptical geometries subjected to tensile stresses, reveal inconsistencies between theoretical estimates and experimental results [8]. Specifically for the ICO project in Venezuela, which aimed to interconnect the Central East and West Phase II gas support systems in the AA1 line (Class AA1 of PDVSA-H-221) [9], a 20″ thick ERW fabricated pipe of 0.375 inches, API 5 L Gr. B carbon steel, is the recommended design. The pipe to be studied here is a straight 600 mm section, with the following design parameters (refer to Fig. 2): A maximum pressure distribution (PD): 275 psig (or 19.33 $\frac{kg}{cm^2}$, or 1.86 MPa), maximum temperature distribution (TD): 110°F (or 43 °C), and corrosion allowance of 0.0625″.

Considering the experience in the industry where a versatile tool is required to be able to give timely results for crack failures in pipes by contracting special studies using commercial software which are based on the finite element [10–13] and in contrast some researchers have defined DCT as the best method for the calculation of the stress estimation factor, it would be worthwhile to see which one is more reliable [14].

This work presents a practical method to estimate the SIF, by comparing the calculations performed on commerical software (ANSYS APDL), with the DCT method, following the work of Barsoum, Hensell and Shaw, for the specific case of an ellipsoidal base, ERW welded gas pipe element, containing a crack. As reproduced in Fig. 3, a key insight arising from the DCT method is that tensions that appear in front of a crack are reproducible, by moving the nodes located at the middle of the sides adjacent to the crack tip, by 1/4 of the original distance could be reproduced the stress which appear in front of the crack.

The Stress Intensity Factor (K_I), relates to differences in the perpendicular displacements of adjacent nodes V_i, as

$$K_I = \frac{E}{8(1-\upsilon)}\sqrt{\frac{2\pi}{L}}[4(V_2 - V_4) - (V_3 - V_5)]. \quad \text{(i)}$$

Here, E is the Young's modulus, or the modulus of linear elasticity, L is the length of the degenerated element, ν is the Poisson's ratio/coefficient, and V_i represents a displacement perpendicular to the fissure plane. This work follows a similar approach as prior works, but aims to minimize any errors.

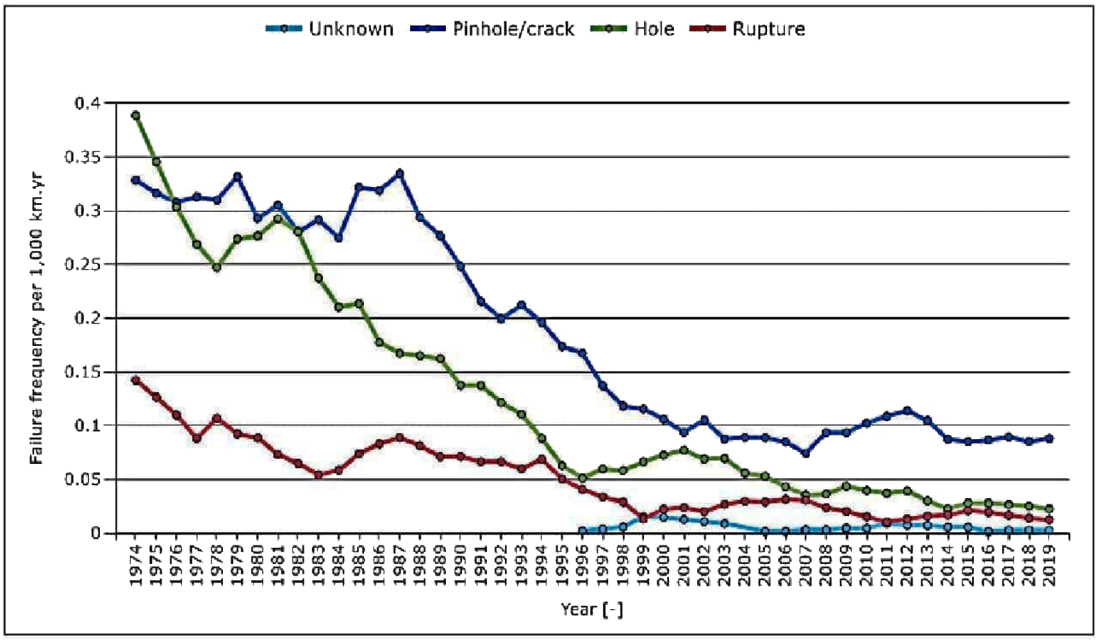

Fig. 1. Frequency of primary failures by leak size.

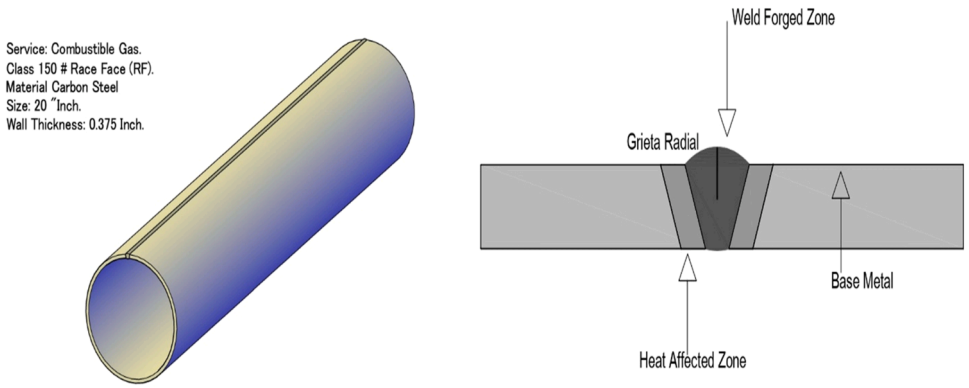

Fig. 2. Schematic of the 6″ ERW pipe geometry for the ANSYS simulation problem. (Figure done By Luis Espinoza).

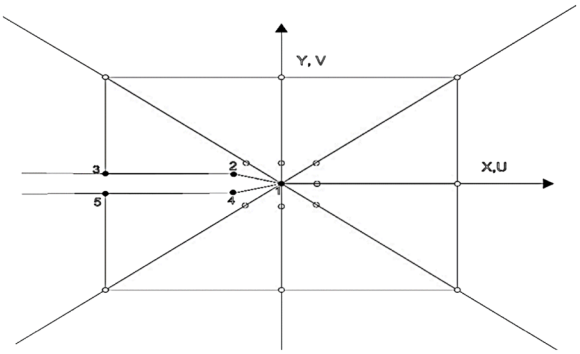

Fig. 3. Degenerated element at a fissure tip, with numbered nodes used to evaluate the fit [8].[12] (Figure done By Luis Espinoza).

There are important approaches concerning this kind studies of comparison between FEM software and the theoric of stress intensity factor, for example a 2D Fracture analysis in a finite plate in tension with a central crack. The problem shows a tabulated solution for the model-I SIF (K_I) available in the literature which the discrepancy estimated is good agreement with ANSYS solution [15].

After the proposal of Hensell and Shaw refered to the studies around the crack tip, Scott and Thorpe [16] reviewed at 80th decade the SIF for elliptic craks where they supported their approachs on the equation of Irwin.[2]

$$K_I = \frac{\sigma_m \sqrt{\pi a}}{E(k)} \left(sin^2\theta + \frac{a^2}{c^2} cos^2\ \theta \right)^{\frac{1}{4}} \quad \text{(ii)}$$

$$E(k) = \left[1 + 1.47 \left(\frac{a}{c} \right)^{1.64} \right]^{\frac{1}{2}} \quad \text{(iii)}$$

Where, σ_m=Applied tensile stress.

$E(k)$= The elliptic integral of the second kind.
a= Crack depth, half the minor axis of a semi-elliptical crack.
c= half surface length or half the mayor axis of a semi-elliptical crack.

They used correction factors evaluated by Holbrook and Dover [17] for finite width plates who make a significant contribution to crack tip stress intensity values calculated but these corrections are essential to correlate cracks propagations data for the same materials in specimens as the compact tension type. It was a theorical and experimemtal approach concerned SIF.

Paris, C, Paul [18] wrote a brief history of the crack tip stress intensity factor where he enfitized its origins, background and development. He did a remembrance from Inglis (1913), Griffith (1924), Irwin (1920–1940), Orowan (1940), Rowe (1955), Lindner (1965), Rice (1968) [19], Elber (1970), Newman (2008), Erdogan(1963) and the contribution the ASTM special committee, the early approaches to sub-critical crack growth, the influence of aircraft U.S. on this matter and other consideration very interesting but at last he summarized that *"For fatigue crack growth matters become even more complex with cicle of loads and beyonds these thougths better analyses will be welcomed here, it means that the studies must be continued in this field"*.

Other approach applied in vessel of chemical industry for example is concerned the works of Livieri and Segala (2016) who derived the equations to estimate stress intensity factors along the whole borders of embedded elliptical cracks in cylindrical and spherical vessels subjected to uniform internal pressure [20]. The modes of crack extension theoric is MODE I: It causes the crack to open orthogonal to the local plane of the crack surface according the point of view of Rice (1968) [21] and Irwin (1960) [22].See Fig. 4.

This approach will contribute to explore real industial case in a gas piping designed for international standards which is used in many power plants, gasducts, uppergrader plants etc.

2. Materials and method

The following is a step-by-step diagram of the methodology See (Fig. 5).

2.1. Pipe material & geometry

To minimize computational penalities and avoid high memory, a symmetric, half-pipe elliptical geometry is chosen (refer to Fig. 6(A))

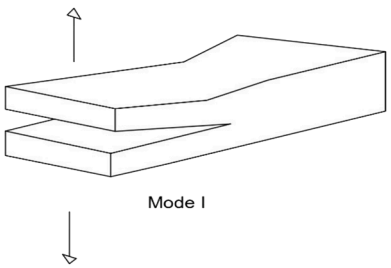

Fig. 4. Mode I of near tip deformation. (Figure done By Luis Espinoza) [23].

[2] In the 1950s Irwin and coworkers introduced the concept of stress intensity factor, which defines the stress field around the crack tip, taking into account. crack length, applied stress and shape factor Y (which accounts for finite size of the component and local geometric features).

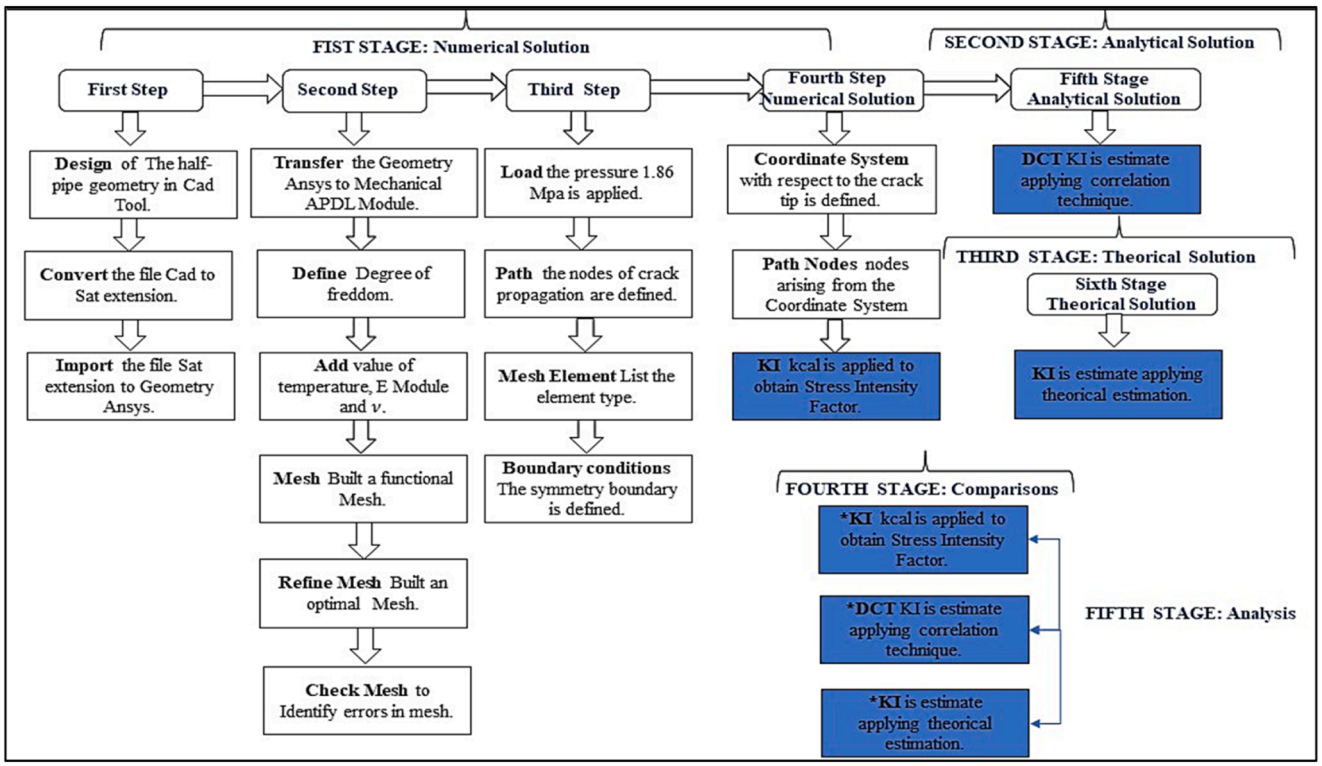

Fig. 5. Step-by-step diagram of study.

[24]. To define the front of the crack, several key considerations must be made. Firstly, as the front part of an actual 3D geometry is being projected to 2D, the line segment OA represents the region, where an eventual analysis would lead to the occurrence of a crack growth, and its consequential propagation. Thus, the calculated stress intensity factor K_I will not be identically perpendicular to the crack, but will actually correspond to the OAz plane, with the $z-$ axis being a plane that lies perpendicular to the crack. Consequently, subsequent crack growth occurs along the direction of K_I, i.e., along the OA line (refer to Fig. 6(B)) [25].

The analysis begins by considering the frontal plane of the crack (Fig. 6(C)), using a Finite Element Method (FEM) approach, implemented as the APDL (Ansys Parametric Design Language) module. A linear elastic behavior of API 5 L Gr. B material (carbon steel) [26] with an eleastic modulus of $2.05 * 10^5$ MPa, and a Poisson's ratio[3] of $\nu = 0.3$ [27] are considered, in accordance with the requisite international standards for an API 5LGr. B material. These mechanical parameters are used to define material features in the ANSYS Finite Element Software Workbench, to ensure optimal solution convergence simulating a real numeric approach of an Industrial situation.[4] The Table 1 gives the mechanical propieties of API 5 L Gr.B material.

2.2. APDL fem procedure & degrees of freedom

The AutoCAD file,[5] containing the geometry, is converted to a .sat extension, and then transferred to the Mechanical APDL work environment (Fig. 7(A)). The degrees of freedom for the type of element, are identifed as UX and UY, as incorporated by the PLANE82 element on ANSYS (Fig. 6(B)).

2.3. Simulation variables, and mesh refinement

The specific working unit USER* system is used in our simulations, the temperature was chosen as 43 °C[6]according the piping class of project. The model material is considered linear, elastic and isotropic, with $E = 2.05 * 10^5$ MPa and $\nu = 0.3$ [29]. An appropriate mesh[7] is defined (Fig. 7(A)), and two iterative refinements were incorporated, to maximize convergence, and rectify any mesh errors. The blue outline corresponds to an element in good condition, while yellow and red correspond to warnings and an evident error, respectively. For our simulation geometry, there were no errors detected (Fig. 7(B)).

2.4. Loading

The internal pressure of 1.86 MPa is applied perpendicular to the pipe on lines. The pressure is icluided in Analysis input parameter in APDL module. This pressure applied is a constant value (Fig. 8(C)).

2.5. Path crack propagation

Several modes are identified to highlight the crack propagation path; for this case the nodes of interest are: 36, 1388 and 1389 (Fig. 8(D)).

[3] Youngś modulus and Poissonś ratio of steel as experimentally determined with standard testing specimen. The assumption for Poissonś ratio ν the material is Isotropic [42].

[4] The mechanical properties of material carbon API 5L Gr B must be defined in worbench chart of Ansys program.

[5] Create model geometry of the problem by constructing lines, arcs, circles, surfaces, etc. This step is normally time consuming especially for complex configuration. An imported CAD model file could help reducing the effort [43].

[6] The temperature must be defined in the Ansys material model (linear isotropic properties for material number). The most needed information in an engineering analysis is the state of temperatures, or displacements and stresses [44].

[7] Mesh properties such as the mesh density and the element shape quality are important factors that affect the solution accuracy and efficiency [45].•USER is refered the units that must be selected in Ansys. To the simulation the KI value will be expressed in $MPa\sqrt{mm}$.

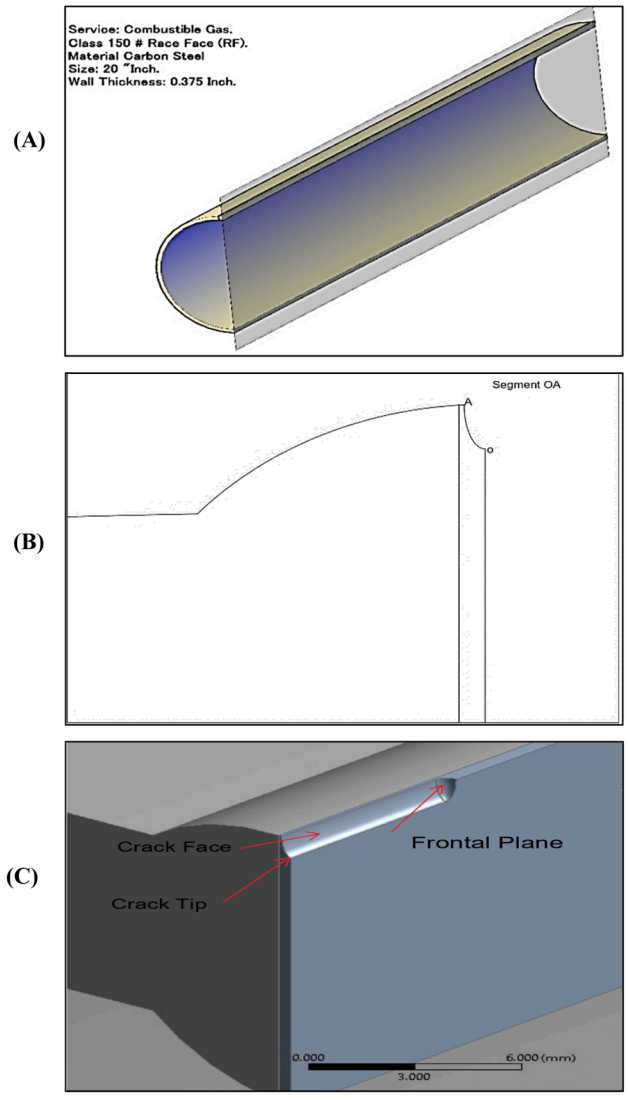

Fig. 6. (A) The half-pipe geometry of interest, after applying the symmetry conditions; (B) the segment OA in the frontal plane of the base crack; (C) 3D geometry of the ellipsoidal base crack. Reproduced from the ANSYS 3D model. (Figures done By Luis Espinoza).

Table 1
Mechanical propieties of API 5 L Gr.B material [26].

Piping Material Specification					
Table 3A – Requirements for PSL 1					
(1)	(2)		(3)		(4)
	Yield Point Min		Tensile Stress Min		Percent of de Elongation min in 2 Inch (50,8 mm)
Grade	Psi*	Mpa	Psi	Mpa	
A25	25.000	172	45.000	310	A
A	30.000	207	48.000	331	A
B	***35.000***	***241***	***60.000***	***414***	***A***
X42	42.000	290	60.000	414	A
X46	46.000	317	63.000	434	A
X52	52.000	359	66.000	455	A
X56	56.000	386	71.000	490	A
X60	60.000	414	75.000	517	A
X65	65.000	448	77.000	531	A
X70	70.000	483	82.000	565	A

* psi = inch per square (Pulgadas al cuadrado) y Mpa = Mega pascal. Units of Stress. Relationship between force and area.

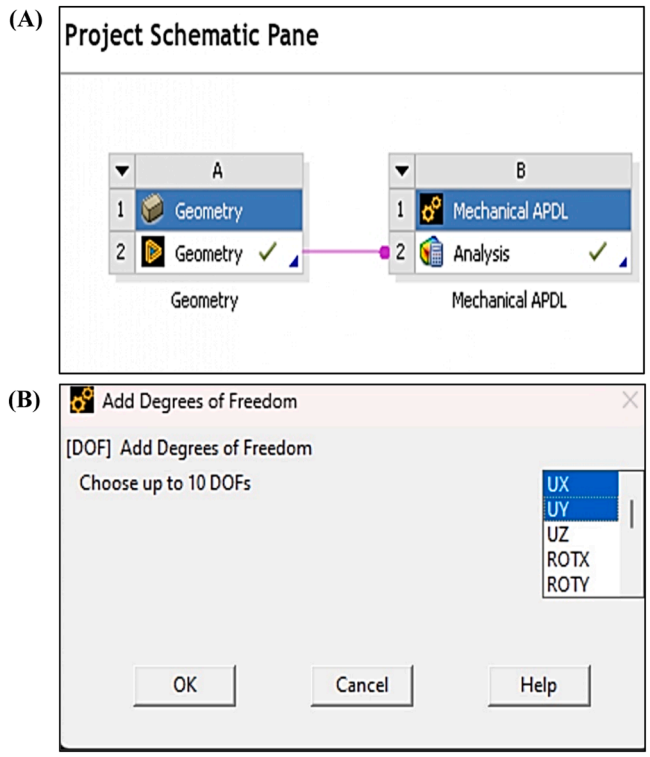

Fig. 7. (A) Workbench environment on ANSYS, used for importing the analysis geometry; (B) degrees of freedom, as identified by the ANSYS 18.2 APDL module [28].

2.6. Mesh element selection and boundary conditions

The ERW weld zone is modelled in ANSYS APDL, using PLANE82 element type. This element is characterized with the following traits: plasticity, slipping, thickening, reinforcements, longitudinal deflection, and deformation capacity. PLANE82 provides accurate results for mixed (quadrilateral-triangular) automatic meshes and can tolerate irregular shapes without as much loss of accuracy. The eight-node elements have compatible displacement shapes and are well suited to model curved boundaries. [X]. The mesh is optimized towards the crack area in APDL, in order to achieve a higher degree of refinement and leads to smaller mesh elements, resulting in better convergence in our results (Fig. 8(A)).

The boundary conditions applied to this model are limited by the degrees of freedom. The symmetry condition is assumed on the crack plane to ensure convergence, thus, the computation is performed for the half-crack. The KCSYM field specifies whether the model is a half-crack model with symmetry boundary conditions, a half-crack model with antisymmetry boundary conditions, or a full-crack model (Fig. 9(B)) [32].

3. Solution technique

3.1. Numerical solution

The K_I value is obtained using the Mechanical APDL work module, starting from the PLANE 82 element, and then, establishing and identifying the tip of the crack, in a suitably defined co-ordinate system (defined with respect to the crack tip). These conditions are captured in

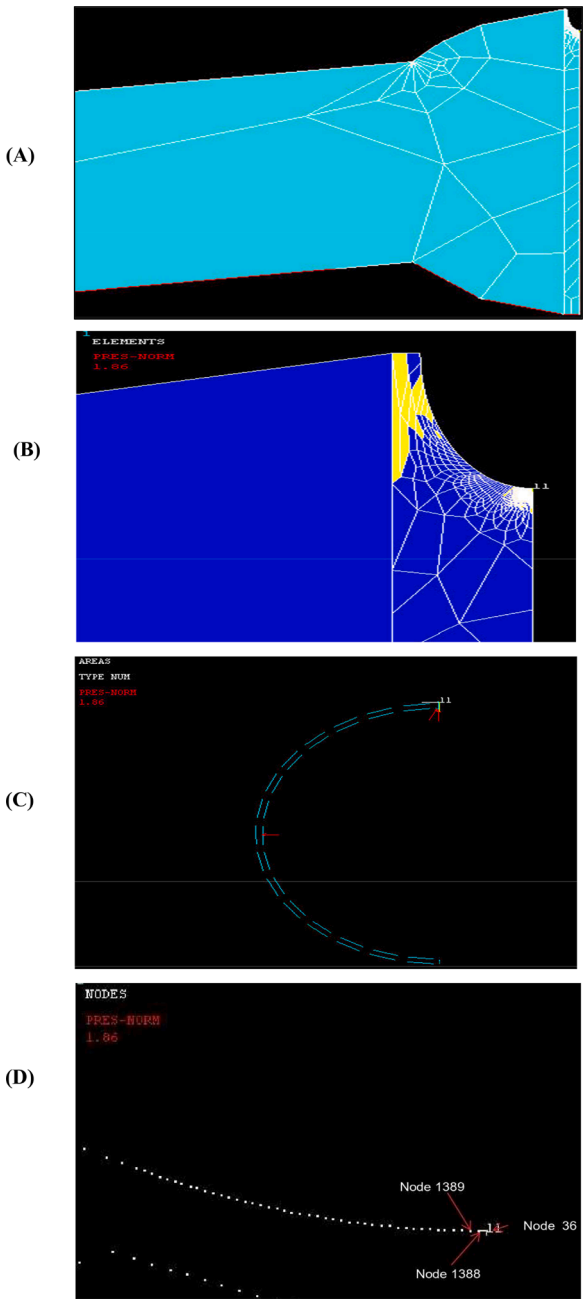

Fig. 8. (A) The defined mesh for the simulation problem, with double refinement and error plane; (B) the mesh shows no errors for the geometry of choice; (C) A pressure of 1.86 MPa is applied perpendicular to the pipelength and (D) crack propagation nodes of interest. Physical properties are defined by ANSYS 18.2 APDL [30,31]. (Figures done By Luis Espinoza).

Figs. 10(A)[8] and 11(B).[9] The ANSYS simulation assumes a static type analysis (for a 1.86 MPa load), with symmetry holding for half the crack geometry, and evaluates a value of $K_I = 0.94$ MPa $\sqrt{\text{m}}$ using the stress intensity factor using KCALC. See Fig. 9(C).

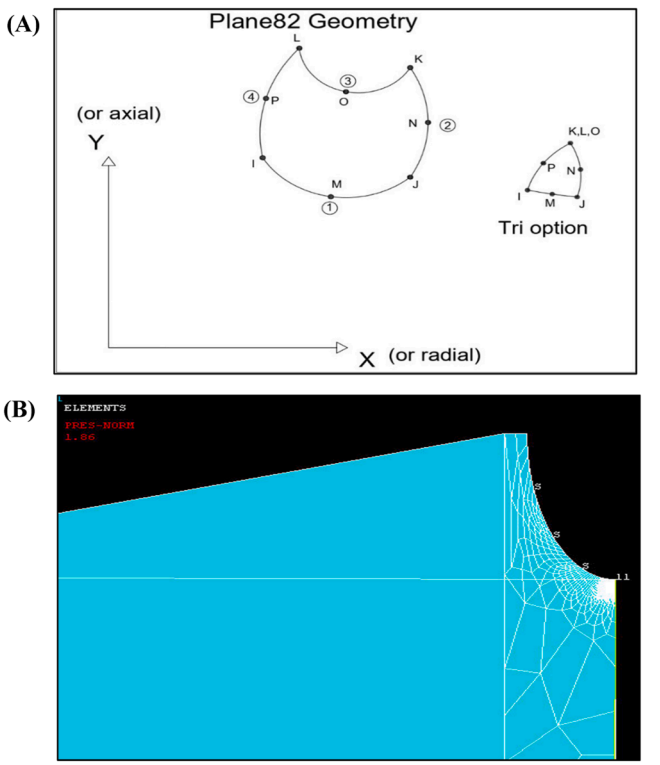

Fig. 9. (A) The PLANE 82 geometry, defined for the ANSYS simulations; (B) implementation of the symmetry boundary condition for the pipe geometry (Letter "S" means symetry). (Figures done By Luis Espinoza).

3.2. *Displacement correlation technique (DCT): analytical solution*

The numerical scheme detailed above, was implemented to simulate a full 20″ piping, in ANSYS APDL, with appropriate degrees of freedom, and input parameters (refer to Table 2) and by applying the Eq. (i).

$$K_I = \frac{E}{8(1-\upsilon)}\sqrt{\frac{2\pi}{L}}[4(V_2 - V_4) - (V_3 - V_5)] \tag{i}$$

But first we must apply the mesh[10] to the area representing the forge of the weld and then we must work out the nodes and apply the Eq. (i).

To conserve computational memory, the mesh is only applied at the weld forged zone.[11] A re-mesh is performed to obtain better computational performance at the area of Fig. 11(A).

Nodes are adjacently numbered, and the location of the next node is obtained by evaluating the differences in displacements of adjacent nodes, to evaluate the stress intensity factor [33]. The work of Barsoum, Hensell and Shaw (the DCT method) are applied on the principal nodes (Fig. 11(A)), while the coordinates of node 32 and the other nodes previously identified (nodes 1,2,3,4, and 5), is simulated on ANSYS (Fig. 11(B)) to evaluate the final value of the stress intensity factor K_I which is $0.70x(10)^{-2}$ $MPa\sqrt{m}$.

[8] This figure is used to define a local crack-tip or crack-front coordinate system with X parallel to the crack face (perpendicular to the crack front in 3-D models) [46].

[9] The basic principles of the finite element method are simple. The first step in the finite element solution procedure is to divide the domain into elements, and this process is called discretization. The elements' distribution is called the mesh. The elements are connected at points called **nodes** [47].

[10] Mesh is one of the mayor steps in preprocessing model [48].

[11] Each zone in the weld area is characterized by a unique microstructure and hence different mechanical properties [49]. This is the area where is focused the analysis to apply DCT.

[12] In the mid-1970s, Barsoum (1974) and Hensell and Shaw (1975) discovered that by moving the mid-side nodes of a quadratic element at the crack tip to quarter point of element side, the singular stress field which occurs at a crack tip could be simulated. Springer Science+Business Media B.V. 2012.

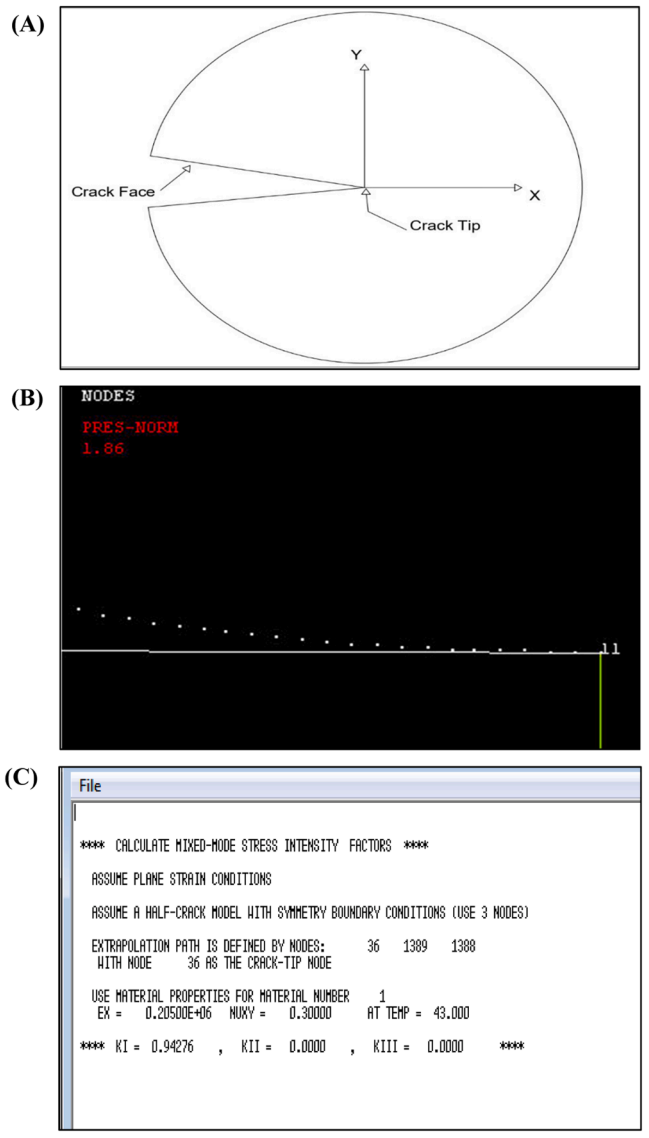

Fig. 10. (A) Definition of the co-ordinate system, with respect to the crack tip, for the simulation; (B) nodes arising from the choice of the co-ordinate system. (C) stress intensity factor using KCALC in APDL module of ANSYS ($0.94x(10)^{-3}$ MPa$\sqrt{m}$). F(igures done By Luis Espinoza).

3.3. Theorical maximum stress intensity factor for elliptical cracks

The theoretical estimation of the stress intensity factor for elliptical cracks is presented below [34,35].

$$K_I = 1.12\frac{\sigma}{\varnothing}\sqrt{\pi a} \tag{iv}$$

$$K_I = 0.5x(10)^{-1} MPa\sqrt{m}$$

4. Results and discussion

As detailed in Section 3, the stress intensity factor is calculated for the half-pipe, by employing **FEM,** followed by mesh refinement (at the crack tip). The final mesh model was performed to a carbon steel material cracked at weld which could be improved more technical of refined mesh, but it will need the most time-consuming in the pre-processing workflow. The simulations were performed with an **academic ANSYS** license, which limits the number of nodal partitions [36].

Successive iterations of the mesh are improved by employing the

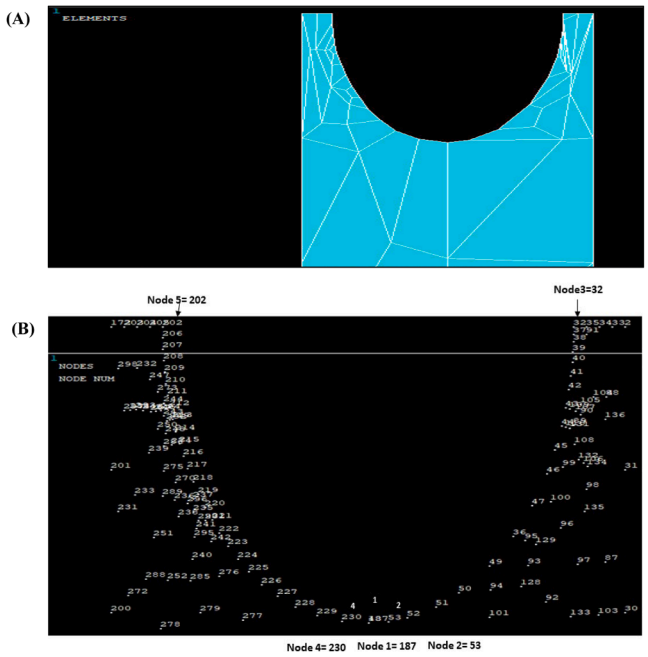

Fig. 11. (A) An initial estimate of the solution mesh, on which the re-mesh is applied twice; (B) solution profile post solution convergence, with key points (nodes 32, 53, 187, 202 and 230) identified. (Figures done By Luis Espinoza).

Table 2
Summary of process parameters used in the simulation.

Simulation Parameters	Estimates
Poisson's coefficient (ν)	0.3
Young's modulus (E), MPa	2.05×10^5
Length of the degenerated element (L)	0.0073
Perpendicular displacements to the fissure V_i = Node 53 – Node 230 (2,4)	0.0001
V_i = Node 32 – Node 202 (3,5)	0.0008
π	3.14159

DCT technique, as detailed in Eq. (i).

The solution technic is an easy way step by step shown at *number 3.1.*

The stress intensity factor is evaluated to be $K_I = 0.94x(10)^{-3}\ MPa\sqrt{m}$ according to the FEM method, while $K_I = 0.70x(10)^{-2}\ MPa\sqrt{m}$ is estimated using the DCT method, using full piping and theoretical estimate of $K_I = 0.5x(10)^{-1}\ MPa\sqrt{m}$ (refer to Table 3).

Despite this, the result obtained for the theoretical technique is far superior to that of the ANSYS 18.2 software and the DCT technique. This

Table 3
$K_I$results comparison.

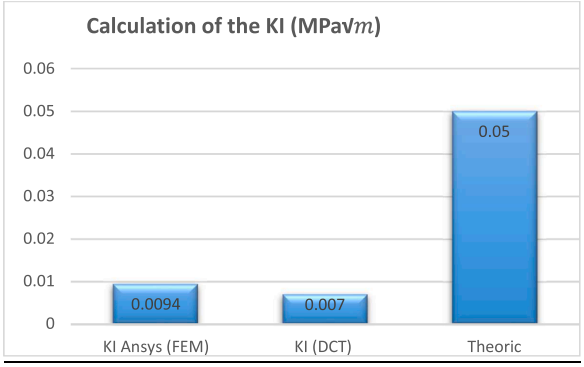

approach is a practical method to compare real industry solutions. That is to say there is a difference in the results obtained by default and not by excess, however; they remain below 1.

The magnitude of stresses at the crack tip are found to be higher when applying the **theoric method**; such comparison may become particularly useful for future theoretical approaches and comparisons.

This would represent a practical way to evaluate the fast studies of FEM elaborated in the Industrial environment for damages in mechanical element in this case a piping with a crack focused at ERW.

4.1. FEM vs DCT technique

The calculation of the K_I for the case study by means of the commercial software Ansys Academic used a standard procedure taking care to comply with all the requirements for this purpose which was estimated at a value less than 1. On the other hand, when applying the correlative displacement technique taking care of the Eq. (i) that represents this technique, a result for the K_I of less than 1 was also obtained. However, when we make the comparison between these two calculation methods, for this specific case of study the correlative displacement technique is lower in terms of absolute value.

Taking as actual value the theoretical value available in the bibliography. (0.05) and applying the following equation.

$$\varepsilon_r = \frac{|\overline{x} - x_i|}{\overline{x}} X100\% \quad \text{(iv)}$$

$\overline{x} =$ the theoretical value.

$x_i =$ *value estimated.*

Comparing these results, a theoretical relative error of **87%** is estimated.

Continuing with the comparisons between FEM and DCT methods against the theoretical calculation, the error rates are presented below.

FEM vs theoric method: Error relative estimated is 81.20%.

DCT technique vs theoric method: Error relative estimated is 86%.

This relative error could be interpreted as an inaccurate analysis, given the accuracy in relation to its actual theoretical value. However, this is a numerical work prone to human error in the presentation of replicating a real case.

It would therefore be useful to conduct this study experimentally to make further comparisons and assess its accuracy.

There is a very close proximity between the FEM calculation and the DCT, however, when compared to the theoretical value, the DCT is closer.

For these cases, it is observed that the stiffness derivative method yields the most accurate results, whereas displacement extrapolation is the easiest method to implement and still yields reasonable accuracy [37].

The theoretical results obtained in this approach show values below unity, being closer to those of the Finite Element Method and the DCT (see Table 3). In the practice of real events in the industry under the FEM it would require a more elaborate analysis and available software licenses, however in the case of the DCT method the steps for its estimation would be less, which would save me man hours of work.

One of the advantages of this application study for industry is that the methods compared are below the theoretical estimation available in the literature.

It would be another scenario if the estimations for this numerical case the obtained values of the FEM and DCT would exceed the theoretical estimations.

4.2. Discussion of limitations

One of the important limitations regarding the application of the finite element software is the student license which is limited to large meshing refinements for example. The license of the ANSYS academic software applied presents the limitation of the number of 512,000 nodes in this analysis [38].

One of the limitations of the Displacement Correlation Technique method is that it there is no traction along the crack faces however this limitation of the quarter-point displacement method was described by Tracey DM [39] but has largely been neglected, as it does not apply to the typical loading conditions in mechanical engineering [40].

In the available literature on this subject some authors have suggested applying correction factors since the regular finite element shape functions do not include the square root terms, which are necessary to accurately represent the displacement field near the crack tip. For this reason, it would be appropriate to make a comparison of a real case for error calculation with correction factor and without correction factor [41].

5. Conclusion

This work estimates the Stress Intensity Factor K_I using both APDL (ANSYS Parametric Design Language) and the Direct Correlation Technique (DCT), for an elliptical base crack, in a longitudinal weld of a 20″ API 5 L Gr. B gas pipe from this approach it is concluded: (1) The difference in K_I values obtained between the two methods is approximately 87%, which shows that despite the advantages of the DCT technique, the accuracy of this method is higher most likely due to the inability of the regular FEM to accurately represent the sharp displacement field near the tip. (2) When comparing the K_I FEM with the theoretical value available in the literature the relative error is 81.20% which can be considered of medium accuracy, however, it remains below unity in absolute terms with a value of 0.0094. (3) When comparing the DCT with the theoretical value available in the literature the relative error is 86% which can be considered not low, however, the comparison between the values obtained 0.007 vs. 0.05 is very sensitive. (4) Both comparisons remain below unity, it is suggested that they can be validated with future experimental studies or use more powerful software licenses that exceed the academic licenses used in this study. (5) Both methods could be practically applied to real industrial cases taking into account their accuracy, since they guarantee me an approximation based on technical concepts, which overcomes industrial proposals without any scientific basis.

Declaration of Competing Interest

The authors declare that they have no known competing financial interests or personal relationships that could have appeared to influence the work reported in this paper.

Data availability

Data will be made available on request.

Acknowledgement

This work was jointly performed at the University of Zaragoza, Spain, and the University of Toronto, Canada.

The present work is not funded.

References

[1] Kim, H. Fatigue behavior of electric resistance welded seams in API -X70 steel. The International Society of Offshore and Polar Engineers: Pohang Korea, 2005, 6 pp.
[2] European Gas Pipeline Incident Data, G. (2020). Gas pipelines incidents. Irland, Denmark, Germany, Spain and others: EGIG.
[3] Toribio, J., González B., Matos, J.C. Review and synthesis of stress intensity factor (SIF) solutions for elliptical surface cracks in round bars under tension loading:

Proceedings of the ICSI 2021 The 4th International Conference on Structural Integrity. USAL. Spain. pp. 1029–1036.
[4] R. Branco, J.D. Costa, F.V. Antunes, Fatigue behaviour and life prediction of lateral notched round bars under bending–torsion loading: CEMUC, Department of Mechanical Engineering, University of Coimbra, Portugal. Engineering Fracture Mechanic, Elseiver, 2014, pp. 66–84.
[5] M. Wojciech, R. Branco, M. Szala, Z. Marciniak, R. Ulewicz, N. Sczygiol, P. Kardasz, Profile and area surface parameters for fatigue fracture characterisation, MDPI, Materials 13 (2020) 3691, https://doi.org/10.3390/ma13173691.
[6] B. Pinheiro, I. Pasqualino, S. Cunha, Fatigue life assessment of damaged pipelines under cyclic internal pressure: pipelines with longitudinal and transverse plain dents, Int. J. Fatig. 68 (2014) 38–47, 2014 Elsevier LtdAll rights reserved.
[7] N.R. Gates, A. Fatemi, N. Iyyer, N. Phan, Fatigue crack growth behavior under multiaxial variable amplitude loading, Frat. Integrità Strutt. 10 (37) (2016) 166–172.
[8] J.M.A Aragón, S. Gutiérrez, Calculations of the intensity factors in cracks initiated in the edges of holes in sheets under stress, Ann. Fract. Mech. 20 (2003) 29–34.
[9] Piping Class Materials, PDVSA H -221, 2015.
[10] M. Thomas, B. Gabriel, A. Schonenberger, R. Eberlein, Simulation and Validation of Residual Deformations in Additive Manufacturing of Metal Parts, Hellion, Institute of Mechanical System, Zurich University of Applied Sciences, 2020, https://doi.org/10.1016/j.heliyon.2020.e03987.
[11] T. Mert, Finite element analysis of effect of weld toe radius and root gap on fatigue life of t-fillet welded joint, in: Proceedings of the Conference of the International Journal of Art of Sciences, Turkey, 2009. ISSN 1943-6114.
[12] C.J. Seok, L. Conghao, Finite Element Simulation of Fatigue Crack Growth The 6th International Forum on Strategic Technology, University of Uslan, Korea, 2011.
[13] K. Ananda, R. Ravichandra, E. Mustaffa, Spur gear crack propagation path analysis using finite element method, in: Proccedings of the International Multi Confenrece of Engineers and Computer Scientists 2012 II, IMECS, Hong Kong, 2012.
[14] L. Banks-Sills, D. Sherman, Comparison of methods for calculating stress intesity factors wth quarter-point elements, Int. J. Fract. 32 (1986) 127–140. Maritinus Nijhhoff Publishers- Netherland.
[15] İ.Y. Sülü, A.O. Ayhan, Sensitivities of two-dimensional fracture problems to the near-tip mesh parameters, Theor. Appl. Fract. Mech. 177 (2) (2012) 207–214. Springer Science Business Media B.V.
[16] P.M. Scott, W.T. Thorpe, A critical review of crack tip stress intensity factors for semi-elliptic cracks, Fatigue Eng. Mater. Struct. 4 (1981) 291–309. Printed in Great Britain.
[17] S.J. Holbrook, W.D. Dover, The stress intensity factor for a deep surface crack in a finite plate, Engng Fract. Mech. 12 (1979) 347–364.
[18] P.C. Paris. (2014). A brief history of the crack tip stress intensity factor and its application, Springer Science +Business Media Dordrech. Parks College of Engineering, Aviation and Technology, With the assistance of Thierry Palin Luc, Arts et Metiers Paris Tech, LAMEFIP, Esplanade des Arts et Metiers, Universite Bordeaux 1, 33405 Talence Cedex, France.
[19] J.R. Rice, G.F. Rosengren, Plane strain deformation near a crack tip in a power-law hardening material, J. Mech. Phis. Solids 16 (1) (1968) 1–12. January 1968Elseiver.
[20] S.F. Livieri, Stress intensity factors for embedded elliptical cracks in cylindrical and spherical vessels, Int. J. Fract. Lettt. Fract. Micromech. 177 (2) (2016) 207–214. Elseiver.
[21] J.R. Rice, Mathematical analysis in the mechanics of fracture, in: H. Liebwitz (Ed.), Chapter 3 of Fracture: An Advance Treatise (Vol 2, Mathematical Fundamentals, Acdemic Press, N.Y., 1968, pp. 191–311.
[22] G.R. Irwin, Structural mechanics, in: Proccedings of the 1st Symposium on Naval Structural Mechanics, 1958", Pergamon, New York, 1960, pp. 557–591 (J.N. Goodier and N. J. Hoff, eds.).
[23] Q.J. Wang, Encyclopedia of Tribology, Springer Science+Business Media, New York, 2013, pp. 134–135.
[24] A.J. Pachoud, P.A. Manso, A.J. Schleiss, Stress intensity factors for axial semi-elliptical surface cracks and embedded elliptical cracks at longitudinal butt welded joints of steel-lined pressure tunnels and shats considering weld shape, Eng. Fract. Mech. EFM (2017), 5498Elseiver.
[25] L. Espinoza, FEM analysis of crack porpagation under fatigue on ERW piping API 5L Gr B of carbon steel, in: Editorial Academica Española, 2019, pp. 38–41.
[26] API, Specification For Line Pipe API 5L, API, Washington, 2004.
[27] Pressure and temperature, PDVSA MDP-01-DP-01, 2015.
[28] ANSYS, help workbench, APDL Module degree of Freddom, 2019.
[29] E.J. Akin, Finite Element Analysis With Error Estimator, Elseiver, Oxford, 2005.
[30] Phan, A. V. Ansys Tutorial. (2010). Ansys tutorial 2-D fracture analysis. Pages 1–14.
[31] D.F.P. Pilkey, Stress Concentration Factors, Wiley, India, 2020, pp. 471–472. Pag.
[32] Boundary conditions (2023). Ansys. Help. Boundary conditions. https://courses.ansys.com/index.php/courses/high-resolution-fe-model-of-bone/lessons/physics-setup-lesson-5-14/topic/4-boundary-conditions.
[33] H. Suárez, N. Sánchez, J. Canizales, A. Toro, Introducción a La Mecánica de La Fractura y Análisis De Fallas, Universidad Autnoma occidente, Colombia, 2008, 52-53-.
[34] D. Broek, The Practical Use of Fracture Mechanics, Klumer Academic Publishers, OH USA, 1988, pp. 51–53.
[35] D. Madier, Practical Finite Element Analysis for Mechanical Engineers, Canada, Éditions Mini Génie, Val-Morin, QC, Canada, 2020, pp. 153–154. Chantal Blanchette.
[36] Leisle Bank, Sherman Dov, Comparison of methods for calculating stress intensity factors with quarter-point elemnts, Int. J. Fract. 32 (1986) 127–140. Martins Nijhoff Publishers. Tel Aviv Israel.
[37] A. Zehnder, Lecture Notes on Fracture Mechanics, Cornell University, 2007, pp. 83–88.
[38] M. Mirzaei, Fracture Mechanics Theory and Applications, Tarbiat Modares University, 2009, pp. 7–36.
[39] P. Fu, S.M. Johnson, R.R. Settgast, C.R. Carrigan, Generalized displacement correlation method for estimating stress intensity factors, Eng. Fract. Mech. 88 (2012) 90–107.
[40] Durán Luis, Varas Gonzalo, Análisis y Desarrollo De La Simulación Termo-Hidraulica De Flujo Multifase En CFD Con ANSYS Fluent, 72, Universidad Politécnica de Madrid, 2017. PP.
[41] D.M. Tracey, Discussion of 'on the use of isoparametric finite elements in linear fracture mechanics' by R.S. Barsoum, Int. J. Numer. Meth. Eng. 11 (2) (1977) 401–402 [11]Li FZ, Shih CF, Needleman.
[42] D. Gross, T. Seelig, Fracture Mechanics with A Introduction to Micromechanics, 3rd Edition, Springer, 2018, pp. 259–260. Pag.
[43] P. Dechaumphai, S. Sucharitpwatskul, Finite Element Analysis With ANSYS Workbench, Alpha Science, Oxford UK, 2018.
[44] Meza, M. & Franco, E. Measurement of the modulus of elasticity in engineering materials using the instrumented indentation and ultrasound technique. Metalurgic Magazine. pp 52–65, 2008.
[45] X Chen, Yijun Liu, Finite Element Modeling and Simulation with Ansys Workbench, CRC Press, New York, 2015.
[46] Vetenskap Och Konst, Introduction to a finite element Analysis program: Ansys. Paper. KTH (Vetenskap och konst) Solid Mechanics, 2002, pp. 1–24.
[47] E. Alawadhi, Finite Element Simulaiton Using Ansys, CRC Press, New York, 2010.
[48] T. Stolarski, S. Yoshimoto, Y. Nakasore, Engineering Analysis with Ansys Software, Elseiver, Oxford, 2006.
[49] Rr. Maksuti, Microstructural changes in the forged weld area during high-frequency electrical resistance welding. International scientific journal "machines technologies materials". Web ISSN 1314-50TX. Macedonia, Issue 5 (2016) 23–26.